The pulsed electro-acoustic technique in research on dielectrics for electrical engineering Today's achievements and perspectives for the future

Olivier Gallot-Lavallée, Virginie Griseri, G. Teyssedre, C. Laurent

The pulsed electro-acoustic technique in research on dielectrics for electrical engineering

Today's achievements and perspectives for the future

Olivier Gallot-Lavallée — Virginie Griseri
Gilbert Teyssedre — Christian Laurent

Laboratoire de génie électrique de Toulouse
Université Paul Sabatier
118 route de Narbonne, F-31062 Toulouse cedex
olivier.gallot-lavallee@grenoble.cnrs.fr

ABSTRACT. *The pulsed electro-acoustic technique is presented to the Electrical Engineering community where it can find many applications, from the development of improved materials for electrical insulation to the control of electrostatic surface discharge (ESD) phenomena. After a short introduction of the space charge problem, we introduce the technique itself and we show how consistent quantitative information can be extracted from this simple method taking examples of dielectrics under field or charged by an electron beam. Non-polar and polar materials are considered and it is shown that space charge and polarization effects can be separated from the spectra analysis. In a last part, we review new perspectives open by this technique to understand and to model electrical transport in dielectrics.*

RÉSUMÉ. *La méthode de l'impulsion électro-acoustique (PEA) est présentée à la communauté du génie électrique où elle peut trouver de nombreuses applications allant du développement de nouveaux matériaux pour l'isolation électrique au contrôle des phénomènes de décharge électrostatique (ESD). Après une introduction au phénomène de charge d'espace, nous présentons la technique elle-même et nous montrons la pertinence des informations obtenues en s'appuyant sur quelques exemples avec des matériaux sous champ, polaires ou non, ou sous irradiation électronique. Dans la dernière partie, nous passons en revue les perspectives ouvertes pour comprendre et modéliser le transport électrique dans les isolants solides.*

KEYWORDS: *PEA, space charge, irradiation, polarisation, dielectrics.*

MOTS-CLÉS : *PEA, charge d'espace, irradiation, polarisation, diélectriques.*

RS - RIGE. Volume 8 – n° 5-6/2005, pages 749 to 772

1. Introduction

Electrical insulations are used in a number of applications, ranging from electrical energy generation and distribution technologies to electronics and space industries. Due to their dielectric nature, these materials are liable to trap electrical charges which can be detrimental for short and long-term performance of the components or systems. A well-known example is synthetic insulation for high voltage equipment where electrical charges appear inside the dielectric by injection from the electrodes, internal dissociation or ion migration from outside (Coelho *et al.*, 1993). These charges that change the internal field distribution and accumulate energy around charged centres are thought to be at the origin of material degradation (Dissado *et al.*, 1997). In space applications, dielectrics placed on satellites can get charged under the effect of charged particles or ionizing radiation up to a level of voltage capable of initiating a fast discharge process leading to harmful interference with the electronic components (Lévy, 2002), so-called electrostatic surface discharge. The same phenomenon is common in electronics, where local accumulation of charges in dielectrics layers can initiate destructive plasma discharge leading to components malfunction. Another quite different aspect of space charge is provided by permanent charged state, so-called electrets, that are used in various applications such as microphone and transducers (Kressmann *et al.*, 1996; Sessler, 2001).

1.1. *Space charge in solid dielectrics*

In a dielectric medium, space charge and electric displacement are related by the Maxwell-Gauss equation. In situations were quantities are dependent on only one spatial coordinate, z, this equation is expressed as:

$$\frac{\partial D(z)}{\partial z} = \rho(z) = \rho_c(z) + \rho_p(z) \qquad [1]$$

where:

D(z) is the electric displacement,

ρ(z) is the total charge density,

$\rho_c(z)$ is the volume density of space charges, defined as real charges, being positive or negative, including surface and bulk charge,

$\rho_p(z)$ is the volume density of bound charges, defined in respect to material polarization P as:

$$\rho_p(z) = -\frac{\partial P(z)}{\partial z} \qquad [2]$$

If the polarization is uniform along the z direction, the total charge is the space charge.

Consideration of the above equations just shows that the main consequence of the presence of space charge in an insulating materials is to change the field distribution imposed by the geometry of the system. Such field distorsions can be very significant. A rough estimation can be made considering a film having a charge density of 1 C/m^3, which is by no way unrealistic considering literature data, uniformly distributed along the thickness direction. For a 1 mm – thick film of relative permittivity of 2, the electric field is null at z = 0 and may reach a value as high as 50 kV/mm which is the order of magnitude of the breakdown field in most of the insulations. Expressed in terms of charged site concentration, 1 C/m^3 corresponds to 1 trapping site per 10^6 atom in a typical solid, that is 1 ppm of impurity which is optimistic or even irrealistic in the domain of technical insulations!

Of course insulations are not uniformly charged and some mechanisms act in the way of a regulation of the electric field. Indeed, if in a specific site of the dielectric the local field exceeds the detrapping field, the space charge is relaxed (trapping sites are depopulated). Hence, a local increase of the field due to the accumulation of charges in another region can be equilibrated through detrapping and transport of carriers. Such processes have been described in the literature in case of unipolar charges (Blaise *et al.*, 1998).

A criterion for the reliability of an insulation can be proposed stating that in any point of the dielectric, the local electric field E(z) must stay below a critical field E_c considered as independent from the spatial coordinate (the breakdown field is a macroscopic parameter that does not account for the heterogeneous character of materials at the microscopic scale). The reliability criterion is expressed as:

$$E(z) < E_c \qquad [3]$$

In the presence of space charge, the field E(z) is the sum of the electrostatic field $E_{es}(z)$ (applied field, constant in case of planar geometry) and of the space charge field $E_{ce}(z)$. The overall electric charges are under the field $E_{es}(z) + E_{ce}(z)$ and the reliability conditions is:

$$E_{es} + E_{ce}(z) < Er \qquad [4]$$

which underlines the necessity to have access to the spatial distribution of the electric field and in some way to forecast this distribution as a function of stressing time.

In another standpoint, the electrical stability of the system must be considered through equilibrium criteria between electric field and space charge. The relevant parameter here is the dynamic of electric stress compared to the dynamic of space charge-related processes.

The above considerations support the interest of developping techniques able to provide the spatial distribution of space charges from which the real distribution of the electric field can be estimated.

1.2. *Historical perspectives of measurements technique*

Until recently, charge storage effect was only probed using techniques capable of yielding information about integral quantities of charges such as thermally-stimulated discharge studies (Laurent, 1999). During the 1980s, a new class of techniques was developed with the ability of disclosing differential data such as the charge distribution along the thickness direction. In most of these methods, a displacement of charges is imposed relatively to the measuring electrodes in a capacitor where the dielectric is placed between two metallic electrodes (Densley *et al.*, 1999; Takada, 1999; Ahmed *et al.*, 1997; Mizutani, 1994). The influence charge on the electrodes is thus modified and this variation is measured in the external circuit. This signal is transformed into a voltage variation across the sample terminals in case of the measurement being performed in open circuit or into a current variation in the case of a short-circuit measurement. The charge displacement is induced by an external perturbation applied to the sample in such a way as to modify its transversal dimension in a non-uniform manner, this last condition being necessary to obtain an electrical response by the deformation of a charged material. In addition, the form and the evolution of the perturbation as a function of time must be known during the measurements.

In practice, the relative movement of the charge with respect to the electrodes can be controlled by a non-uniform expansion of the medium induced by a local temperature elevation on one of the sample sides (methods known as thermal (Bloss *et al.*, 1994; Lang *et al.*, 1986; Nothinger *et al.*, 2001; Toureille *et al.*, 1988)) or by the generation of a pressure wave (methods known as acoustic (Sessler, 1987; Satoh *et al.*, 1997; Laurenceau *et al.*, 1977)). These methods can take different names depending on the type of stimulation applied, thermal or acoustic, and its shape. Finally, there is a third method known as the Pulsed Electro-Acoustic technique (Maeno *et al.*, 1988, 1999, 1985) based on a different principle. Here, a voltage pulse is applied to the sample to provide stimulation. The induced electric field produces on each existing charge a Coulomb force. Acoustic waves are thus engendered by the exchange of momentum between the electrical charges, bound to the atoms of the dielectric, and the medium. These waves are then detected by a piezoelectric sensor and recorded as function of time to provide the basis for the reconstruction of a one-dimensional distribution of the space charge bulk density.

In the 1990s, these techniques matured and were routinely used in labs and industrial sites (Fukunaga, 1999). Among them, pressure wave propagation (acoustic) and thermal methods became popular in Europe and North-America (Nothinger *et al.*, 2001; De Reggi *et al.*, 1992, Bloss *et al.*, 1997, Sessler *et al.*,

1992), whereas the pulsed electro acoustic technique was preferred in Japan (Li *et al.*, 1994; Hozumi *et al.*, 1999). In spite of the fact that the situation is currently undergoing a change (Montanari *et al.*, 1998; Alison, 1998; Morshuis *et al.*, 1997) the PEA method is still less well-known in Europe. The objective of this paper is to give a short presentation of its measurement principle and data treatment and to present some results on charged samples obtained under very different conditions showing the versatility of this method and its consistency, considering specially case study pertaining to the field of Electrical Engineering. In a last part, we shall describe the expected future developments and applications of the PEA method in this field of research.

2. Description of the Pulsed Electro-Acoustic method

2.1. *Principle*

The PEA measurement principle is given in figure 1. Let us consider a sample having a thickness d presenting a layer of negative charge σ at a depth x. This layer induces on the electrodes the charges σ_d and σ_0 by total influence so that:

$$\sigma_d = \frac{-x}{d}.\sigma \quad and \quad \sigma_0 = \frac{x-d}{d}.\sigma \qquad [5]$$

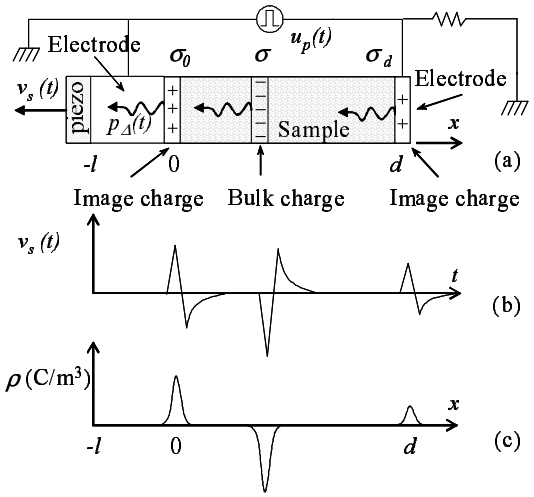

Figure 1. *Principle of the PEA method. (a) Charged regions give rise to acoustic waves under the effect of a pulsed field. (b) As a consequence the piezoelectric sensor delivers a voltage $v_s(t)$. (c) An appropriate signal treatment then gives the spatial distribution of image and internal charges*

Application of a pulsed voltage $u_p(t)$ induces a transient displacement of the space charges around their positions along the x-axis under Coulomb effect. Thus elementary pressure waves $p_\Delta(t)$, issued from each charged zone, with amplitude proportional to the local charge density propagates inside the sample with the speed of sound. Under the influence of these pressure variations, the piezoelectric sensor delivers a voltage $v_s(t)$ which is characteristic of the pressures encountered. The charge distribution inside the sample becomes accessible by acoustic signal treatment. The quantification of the measurements passes by a referencing procedure whose description will follow.

2.2. *Theoretical analysis*

Let us consider a sample with a volumic charge distribution ρ as shown in figure 2 and divide it in a set of rigid charged layers of thickness Δx and homogeneous charge density. The force $f_\Delta(x,t)$ representing the dynamical component of the force exerted on each layer of the x-axis due to the coupling of the electric field pulse e(t) with the charge is thus expressed as:

$$f_\Delta(x,t) = \rho(x).\Delta x.S.e(t) \qquad [6]$$

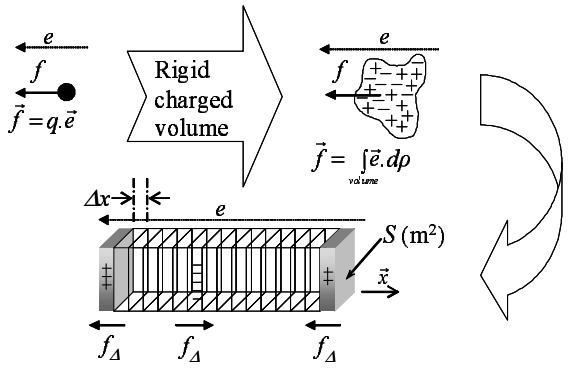

Figure 2. *Model for the equation set up*

The pressure waves, obtained dividing f by the surface S of the electrode, reaches the piezoelectric detector without changing shape with the following hypothesis: the acoustic wave propagates in a homogeneous and perfectly elastic medium, *i.e.* attenuation and acoustic dispersion factors are nil in Fourier space (Li *et al.*, 1995; Alison, 1998; Maeno, 1999). The delay between wave production and detection is directly dependent on the speed of sound characteristic of each material traversed, being designated by vp for the sample and ve for the electrode of

thickness l adjacent to the piezoelectric sensor. The pressure seen by the detector is as follows:

$$p_{\Delta}(x,t) = e(t - \frac{l}{v_e} - \frac{x}{v_p}).\rho(x).\Delta x \qquad [7]$$

The pressure exerted on the sensor by the entire set of elementary layers is obtained thereafter by the summation:

$$p(t) = \int_{-\infty}^{+\infty} p_{\Delta}(x,t) = \int_{-\infty}^{+\infty} e(t - \frac{l}{v_e} - \frac{x}{v_p}).\rho(x).\Delta x \qquad [8]$$

Note that the electric field e is nil outside the dielectric, *i.e.* $\forall$ x $\notin$ [0,d].

Setting $\tau = x/v_p$ and $\rho(x) = \rho(\tau.v_p) = r(\tau)$ gives:

$$p(t) = v_p \int_{-\infty}^{+\infty} e(t - \frac{l}{v_e} - \tau).r(\tau).d\tau \qquad [9]$$

The form of equation [9] being that of a convolution, it can be simplified by the application of Fourier transform:

$$P(\nu) = \mathrm{F}[p(t)] = v_p.R(\nu).E(\nu).\exp[-2i\pi\nu.\frac{l}{v_e}] \qquad [10]$$

As for the piezoelectric sensor, its output $v_s(t)$ and its input p(t) can be expressed by a convolution law such as, in the Fourier space:

$$Vs(\nu) = H(\nu).P(\nu) \qquad [11]$$

where H(ν) is the characteristic transfer function of the piezoelectric sensor, encompassing the entire set of the amplifier and the waveguide, from the practical point of view.

At this stage of argument, one unknown remains to be eliminated, H(ν), for obtaining R(ν)… It is unravelled by using a reference signal.

The referencing procedure illustrated in figure 3 has the role of eliminating the unknown H(ν) which is the characteristic transfer function of the piezoelectric sensor and related electronics. For that we consider a sample free from charges to which a constant voltage U is applied. The surface density of the charge (capacitive charge) on the electrodes is then:

$$\sigma_1 = \frac{\varepsilon_1 . U}{d_1} \qquad [12]$$

Here and in what follows, the index 1 refers to calibration data.

With the hypothesis that the capacitive charges due to the pulsed field e are negligible compared to all others ($u_p << U$), the pressure thus created by the electrode nearest to the sensor is expressed as:

$$p_1(t) = \sigma_1 . e(t - \frac{l}{v_e})$$

$$\Rightarrow \mathrm{F}[p_1(t)] = P_1(\nu) = \sigma_1 . E(\nu).\exp[-2i\pi\nu . \frac{l}{v_e}] \qquad [13]$$

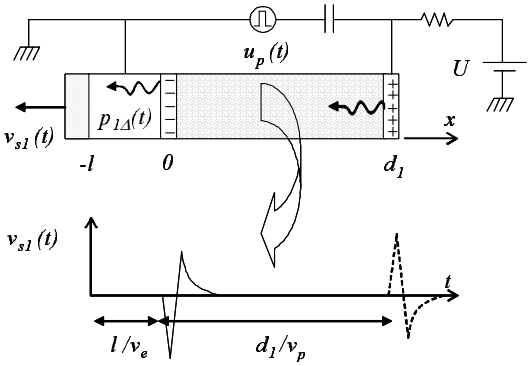

Figure 3. *Principle of the reference measurement. The reference signal is that produced by the capacitive charges located on the electrode adjacent to the piezoelectric sensor (solid line)*

Piezoelectric conversion properties being always the same, we have:

$$Vs_1(\nu) = H(\nu).P_1(\nu) \qquad [14]$$

from which H(ν) is extracted.

Combining equations [10], [11], [13] and [14], we obtain the expression of F[ρ(x)] as:

$$R(\nu) = \frac{\sigma_1}{v_p} . \frac{Vs(\nu)}{Vs_1(\nu)} \qquad [15]$$

Now ρ(x) is obtained by the inverse transform of Fourier, such as:

$$\rho(x) = \mathrm{F}^{-1}[R(\nu)] = \mathrm{F}^{-1}\left[\frac{\varepsilon_1 . U}{v_p . d_1} \cdot \frac{V_s(\nu)}{V_{s1}(\nu)}\right] \qquad [16]$$

As such, the charge profile determination passes by two measurements: the first gives us $v_s(t)$ to be converted to $V_s(\nu)$ by Fourier transform; the second (reference) gives us $v_{s1}(t)$ to be converted to $V_{s1}(\nu)$.

2.3. *Practical details*

A presentation of the test bench is shown in figure 4. Transient field excitation is provided by a short pulse (5 ns) voltage generator. An HVDC supply (maximum voltage, typically 30 kV, being limited by the geometry of the cell), is used in order to perform the reference measurement (low voltage) and to apply DC electric stress to the sample during measurement. A piezoelectric sensor (PVDF 9 µm) detects the incident acoustic waves, and then provides a characteristic voltage.

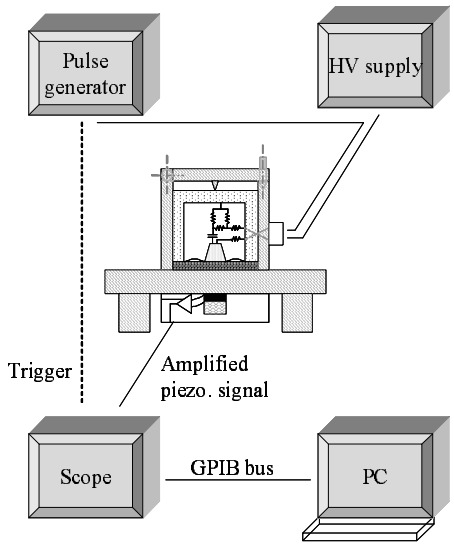

Figure 4. *General presentation of the PEA test bench*

The output of the piezoelectric sensor is amplified by a device (50 dB 0.1-500 MHz) located at the proximity of the sensor (shielded area) and then acquired by a numerical oscilloscope (500 MHz of sampling rate). The signal is processed by a PC regarding the physical equations exposed above.

Details of the PEA cell are given in figure 5. A coupling capacitance (250 pF) provides a galvanic insulation between the DC supply and pulsed signal generator and a resistance (5 MΩ) is inserted in series with the HV circuit in order to limit current. Matching impedance takes place close to the electrode in order to optimize electrical wave transfer from the pulse generator.

The top electrode is made of copper and a semi-conducting material (carbon black reinforced polymer) is placed in contact with the sample in order to have a good acoustic impedance matching. The bottom electrode is made of aluminium. It has a large thickness and so acts as delay line between the acoustic signal and the electrostatic noise provided by the pulse generator. A PMMA sample is used to hold the piezoelectric sensor on the lower electrode with a good acoustical impedance matching. Table 1 contains the essential features of our test-bench experimental characteristics.

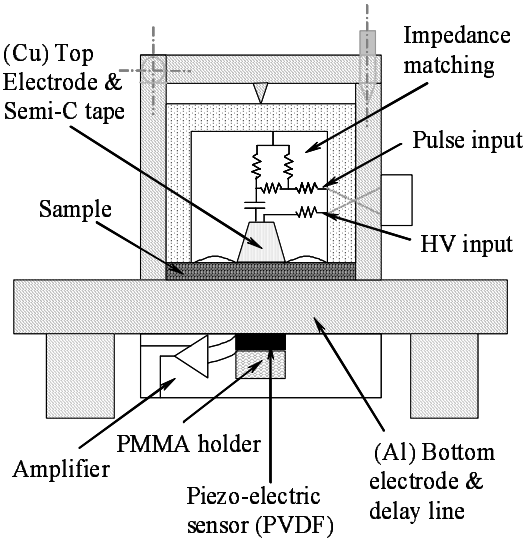

Figure 5. *Details of the PEA cell*

Table 1. *Experimental characteristics of the test bench*

Voltage pulse	50 V-2 kV; 5 ns; 300 Hz-2 kHz
Number of averaged responses	≥ 1000 taking 10 s
Direct Current polarization	0-30 kV
Test bench sensitivity	0.1 C/m³
Spatial resolution	10 µm
Sample thickness	0.1-1 mm

2.4. *Measurement and experimental error*

A film of epoxy resin of 485 µm thickness and relative permittivity $\varepsilon_r = 3.5$ was subjected for a short instant to an applied voltage of 3 kV for the purpose of acquiring a calibration signal. The charge and field profiles obtained are plotted in figure 6. They are characteristic of a space charge-free dielectric under voltage (capacitive charge only). The potential distribution is linear within the insulation and reaches the expected value of 3 kV on the right electrode, and we find from integration within the regions defined by vertical lines on either side of the sample a quantity of induced charge, *i.e.* a capacitive charge, $\sigma_1 = \sigma_2 = 190\ \mu C/m^2$ in very good agreement with that deduced from equation [11]: $\sigma = \varepsilon U / d = 192\ \mu C/m^2$.

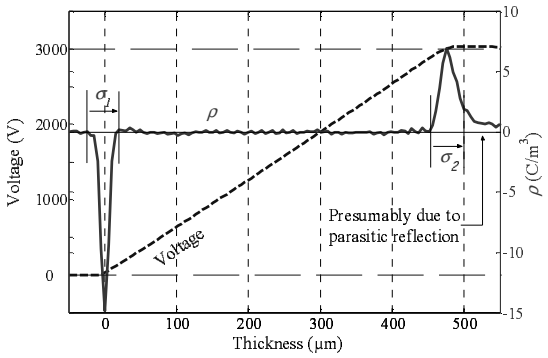

Figure 6. *Charge (solid line) and potential (dotted line) profiles in an epoxy resin polarized for a short instant under 3 kV*

The above observations validate PEA measurements for a material under field. However, it is worth stressing that the shape of the image charge profile is not the same for the two electrodes, being broader on the electrode the further away from the detector (anode, right-hand side), *i.e.* for the signal related to acoustic waves having travelled through the whole insulation thickness. According to (Maeno, 1999) and (Alison, 1998), three types of error can be identified, in addition to acoustic dispersion and/or multiple scattering of the acoustic waves: i) a random error due to noise within the experimental system, which is eliminated with signal averaging carried out in PEA method; ii) systematic errors in the signal calibration parameters, e.g. sample thickness d_1, applied voltage U, velocity v_p and dielectric permittivity ε_1 (see equation [12]), and so for the test sample; iii) errors due to the numerical processing of the signal, which is depicted in figure 7, and to the detection and acquisition system (Jeroense, 1997).

Indeed, the signal passes by three principal filters, provided by the piezoelectric sensor, the amplifying circuit and the oscilloscope. It is thereafter digitized and processed numerically, through steps using Gauss and Wiener functions aimed at

limiting the frequency range of the signal spectrum and avoiding division by zero in the Fourier space, respectively. The effect of Gaussian filter processing on space charge spreading is modeled in figure 8. Usually, noise is acceptably reduced with 1/g = 2 as Matlab Gaussian filter parameter.

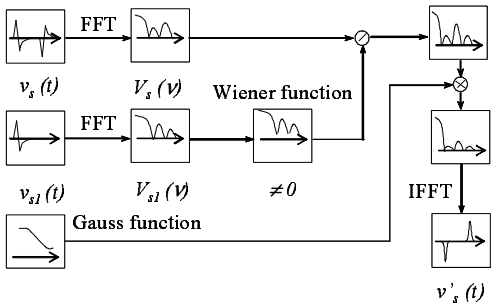

Figure 7. *Synoptic of the signal processing implementation (Jeroense, 1997)*

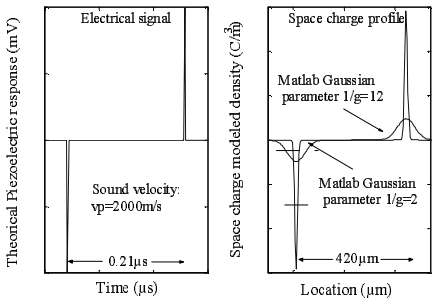

Figure 8. *Effect of a numerical processing by a Gaussian filter on space charge profile spreading*

Typically, for a situation of 2 ns of sampling rate and 2 000 m/s of sound velocity, the spreading is of the order of 20 µm. Using l/g = 12, the peak width at mid-height would be around 96 µm.

3. Case study

3.1. *Non polar dielectric under dc field*

A 150 µm-thick crosslinked polyethylene (XLPE) film has been subjected to polarization/depolarization cycles of 5 min/5 min, for fields in the range 4 to

100 kV/mm, the purpose being to determine the behavior of space charge as a function of field. Figure 9 shows profiles obtained after 5 min of depolarization following polarization at various values of field level. A profile obtained in volt-on at low field (field = 4 kV/mm) is also shown for the purpose of defining the position of the electrodes (essentially capacitive charges are seen in that case).

From 10 kV/mm onwards, XLPE accumulates charges of the same sign as that of the charge on the adjacent electrode, *i.e.* homocharges are injected. This behavior is best seen at low field on the cathode side. When the field increases, charge accumulation at both electrodes becomes clearer and these charges penetrate deeper in the insulation. At 60 kV/mm the positively and negatively charged regions meet each other, giving rise to a situation where the two kinds of carriers may coexist. Recombination processes are likely to occur in this field range. In fact it has been shown that 60 kV/mm corresponds to the onset field for electroluminescence (EL) detection reflecting recombination phenomena in the material (Tardieu, 2003).

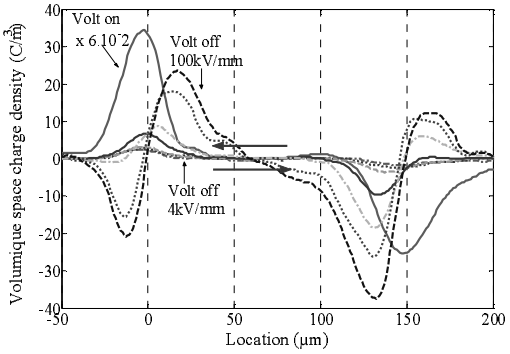

Figure 9. *Space charge profiles of a XLPE sample subjected to successively increasing electric fields*

3.2. *Polar dielectric under dc field*

An epoxy sample similar to the one used in the experiment reported in section 2.4 was submitted to a field of 40 kV/mm applied during 1 hour, and then under short-circuit conditions of equivalent duration. The rise time of the voltage was set to 1 kV/s. PEA spectra were recorded every 20 sec. The amplitude of the PEA pulse was set to 300 V, giving a pulse field of 0.6 kV/mm.

Profiles obtained in the vicinity of the cathode are shown in figure 10 as a function of time, both during polarization and depolarization, allowing following the kinetics of charge build-up and decay. We can observe that the amplitude of the image charge in Volt-on decreases and the position of the maximum moves towards

the bulk with time. In Volt-off, the polarization charge decreases quickly and the bulk charge is practically released after one hour of depolarization.

The objective here is to separate bulk charge, influence charge and slow polarization contributions to the PEA signal. If we stay on the previous hypothesis that is to say the charge is enough confined on the respective electrodes, then we can write the following relation between the bulk charge and the related image charge, the index *K* referring to the cathode:

$$Qb_K \approx -Qim_K \qquad [17]$$

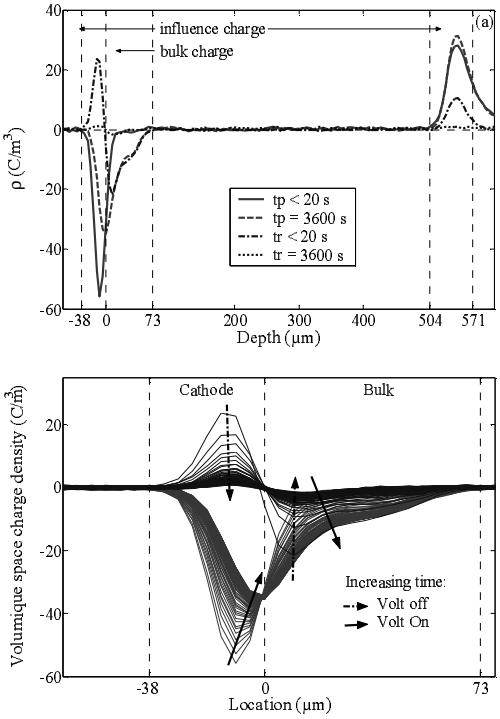

Figure 10. *Space charge profiles during polarization/relaxation cycle. Top a global view on the 500 μm of sample thickness. In bottom a zoom on cathode area with the recorded profiles each 20 s*

The influence charge, Qi_K, is a superposition of the image charge, Qim_K and of the polarization charge Qp_K:

$$Qi_K = Qp_K + Qim_K \qquad [18]$$

The access to the dipolar processes (slow polarization) from the space charge profiles then becomes possible considering the following relation:

$$Qp_K = Qi_K + Qb_K \qquad [19]$$

We understand by Qim_K, the cathodic charge influenced by the associated homocharge, Qb_K. Qp_K is used here to describe the influence charge on the cathode due to the polarization phenomenon. Finally, Qi_K indicates the total charge on the cathode created by influence.

We have integrated the net charge, for each of the regions bounded by dotted lines in figure 10, and the dynamics of build-up and relaxation of the charge is represented in figure 11 for the cathode region of the un-metallized sample.

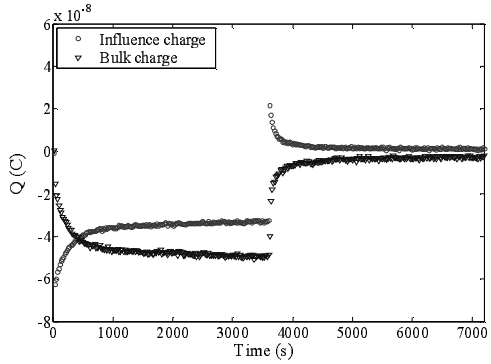

Figure 11. *Dynamic of net charge variation during a polarisation/relaxation cycle at the cathode. Quantities were integrated in the regions limited by dashed lines in figure 10 and are relevant to a 0.5 cm² area of the sample*

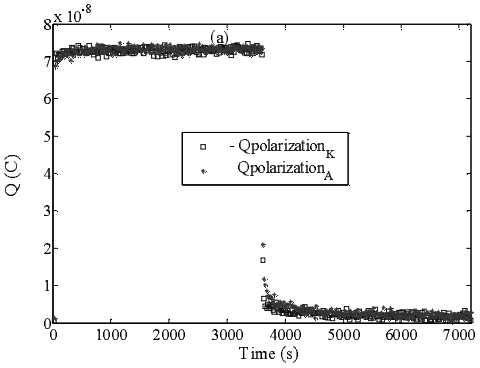

Figure 12. *Dynamic of the polarization charge during a polarisation/relaxation cycle. Quantities are relevant to a 0.5 cm² area of the sample*

We notice that the variations of charge are important in the first moments of the application of the stress or after the short circuit, then it becomes much slower after the first 20 minutes. This is visible in an almost symmetric way for the influence charge and the bulk charge in figure 12, thus revealing that the variation in influence charge is primarily due to the build-up of the injected charge (weak contribution of delayed polarization).

3.3. *Electron beam irradiated dielectrics*

An epoxy resin, of the same nature as that used in section 3.2, was irradiated by a monoenergetic electron beam at 200 keV for a period t = 240 s with a flux J = 5 μA/m^2 under secondary vacuum conditions. The charge and field profiles obtained 5 h after irradiation are represented in figure 13. In the case where the sample irradiation flux is under control, as it was here, it becomes trivial to estimate the implanted charge quantity in the volume probed by the PEA set-up, the effective electrode surface being S = 56.7 mm^2:

$$Q = J \cdot t \cdot S = 68\,\text{nC} \qquad [20]$$

The internal charge density obtained from integration of the measured profile is 55 nC. This is in good agreement with that deduced from equation [20], given the fact that not necessarily all the charge produced by the beam is implanted and that part of the implanted charge may have disappeared, through conduction during the time lag of 5 h elapsed between the irradiation step and the measurement step. In this respect, it was observed that the internal charge density was halved 25 h after irradiation relatively to its value at 5 h. The dynamic of charge release can be followed e.g. through surface potential measurement. In the absence of charge compensation, *i.e.* build-up of image charge at the surface, the surface potential is expected to be directly related to the internal charge distribution. However, when exposing the sample to air after charge implantation, the surface potential decays, not because internal charges are evacuated, but just because image charges build up due to the environment, like if the sample was short-circuited. In this respect, internal space charge measurement appears as much more informative than surface potential measurement, all the more than in-situ measurement of profiles within the irradiation chamber is now achievable (Griseri *et al.*, 2004).

We carried out the same experiment as previously using a stronger irradiation energy of 300 keV and the profiles obtained subsequently are shown in figure 14. One observes a deeper penetration depth of charge in comparison to figure 13, and it is noticeable that the image charge on the right electrode increases accordingly.

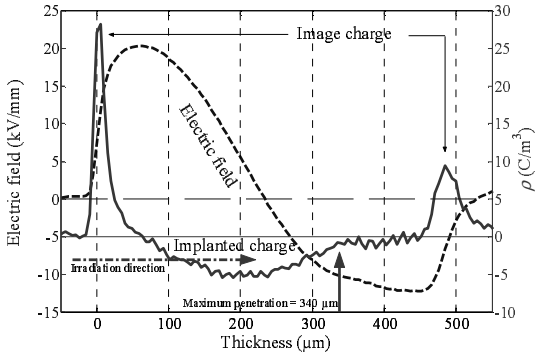

Figure 13. *Charge (solid line) and potential (dotted line) profiles in an epoxy resin obtained 5 h after charging under electronic beam at 200 keV*

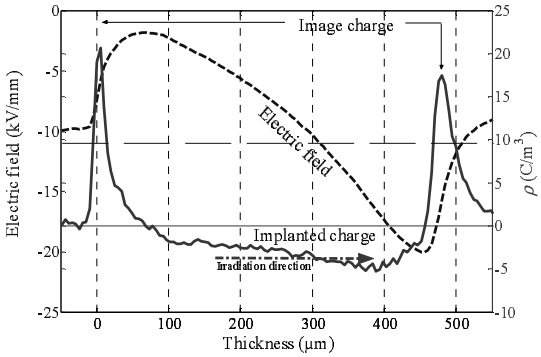

Figure 14. *Charge (solid line) and potential (dotted line) profiles in an epoxy resin obtained 5 h after charging under electronic beam at 300 keV*

Now it is possible to estimate the electron penetration depth in the dielectric using an appropriate model. We have thus estimated this depth using a software called ESTAR (Estar, 2003) which is given to the public by the National Institute for Standards and Technologies (NIST). The chemical formulation of epoxy-based resins being particularly complex, we carried out the calculation assuming the following atomic concentrations: O: 17.5%; H: 17.5%; C: 60%; N: 5% and the density of our epoxy resin as 1.23 g/cm^3. Figure 15 shows the maximum penetration depth of electrons as a function of energy of electrons. The maximum penetration depths estimated by the model are 332 µm and 625 µm for 200 keV and 300 keV energies, respectively. The former compares favourably with experimental measurements (340 µm from figure 13), whereas for the latter, the penetration depth

exceeds the sample thickness. However, it can be inferred from figure 14 that electrons have probably crossed through the right-hand electrode, the presence of the image charge preventing any fine determination of the internal charge close to the electrode.

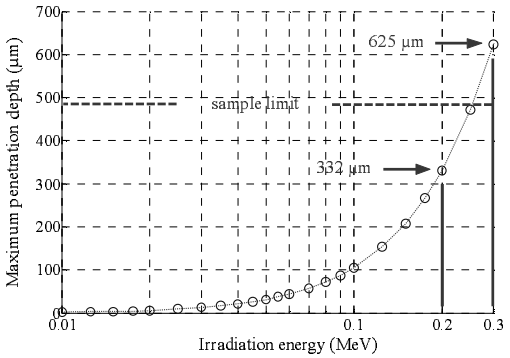

Figure 15. *Maximum penetration depth of electrons as a function of their energy as estimated using the ESTAR model (Estar, 03) and the following characteristics for epoxy: density = 1.23 g/cm3; % at. O: 17.5; H: 17.5; C: 60; N: 5*

4. Development of the technique and perspectives for the future

4.1. *Development of the technique*

The developments of the PEA method have been driven by scientific and technical requirements.

On the scientific side, there is a strong pressure to perform high speed PEA measurements enabling the study of the dynamics of the space charge under time-varying electrical stresses such as ac or impulse voltages. This requires a time resolution for a single measurement that is suitable to get several spectra within a short time. There is also the need to increase the sensitivity and the spatial resolution of the PEA in the direction of the acoustic wave propagation in order to perform measurements on thinner films. Measuring systems having a lateral resolution (spatial resolution in a direction perpendicular to the propagation of the acoustic wave) are also needed since the information is averaged in a plane with conventional PEA, and there is question about the isotropy of the space charge in this plane. Another improvement concerns the ability to perform simultaneously with the space charge, a complementary measurement in relation with the transport process giving additional information, in a large variety of experimental situations. Finally, some special configurations have been developed for detecting the space charge implanted in a dielectric by a particle beam.

On the technical side, the pressure was towards measurements on components and systems rather than on materials. This has been achieved in a large number of cases. Complex materials were also considered which involves modelling of the acoustic propagation in systems having interfaces of different acoustic impedances. Finally, a miniaturized version of the PEA was proposed for on-site monitoring.

Time resolution: the best time resolution achieved so far for a single measurement is 10 µs (Fukuma *et al.*, 2002). This has been realized by using a high speed switching semiconductor able to deliver high voltage pulse at a frequency of 100 kHz, and associated recording method using digitizing oscilloscope (1 ns sampling rate and 1 Mb in memory). Measurement of space charge distribution has been carried out with such time resolution during the application of a high voltage pulse of 1 ms in duration.

Signal to noise ratio – Sensitivity: the best sensitivity achieved for the method is about 0.1 $C.m^{-3}$, which mainly depends on the noise reduction level. This level corresponds typically to one electric charge per 10^{11} atoms.

Spatial resolution in the direction of the acoustic wave: the spatial resolution has been improved by reducing the width of the voltage pulse used to probe the space charge (as short as 2 ns) and the thickness of the piezoelectric sensor. The best achieved spatial resolution is 2 µm (Maeno *et al.*, 1996).

3D-spatial resolution: measurement with a 3D-spatial resolution has been obtained by using multiple-piezoelectric sensors of small surface and multiplexing techniques for analyzing the data (achieved resolution of the order of 1 mm in the lateral direction) (Fukuma *et al.*, 2004). By using acoustic lens, a lateral resolution of 500 µm and a resolution in depth of 12 µm have been obtained (Maeno *et al.*, 2001).

Combined measurements: external current (Fukuma *et al.*, 1999) and electroluminescence (Miyake *et al.*, 2004) measurements have been performed simultaneously with space charge detection enabling respectively the separation between the conduction and displacement components of the current, and the correlation between space charge distribution and dissipative processes as seen through the emission of photons.

Measurement under electron irradiation: a specific PEA configuration has been developed to follow the charge implanted in a dielectric under an electron beam (Griseri *et al.*, 2004). This needed a different architecture of the PEA since a surface of the sample has to be exposed to the charging beam.

Non-contact mode: measurements have been achieved in the so-called "non contact mode" where one surface of the film is "free" from any contact with an electrode. In that case, an air gap exists between this surface and the measuring electrode and the acoustic wave propagates within the air gap. This configuration is useful when charge released has to be avoided from one electrode (Maeno *et al.*, 2004).

Measurements on complex materials, components and systems: laminated or multi-layered dielectrics, micro-and nano-composites dielectrics were considered. Measurements have also been performed on components and systems such as power cables (up to 550 kV) (Hozumi *et al.*, 1994), capacitors, printed circuit boards (Fukunaga *et al.*, 1998). A good summary of the industrial applications of the PEA method can be found in (Fukunaga, 1999). PEA miniaturisation for on-site monitoring: A portable, miniaturized version of the PEA has been developed for on-site monitoring (Maeno, 2004).

4.2. *Perspectives for the future*

The development of this versatile tool opens several ways of research in different domains. The most obvious is pertaining to material research where the quantity of space charge in a given material for a given application must be controlled. The PEA provides a direct feedback between chemical, physical and structural properties of a dielectrics and its ability to store or transport space charge under given electrical conditions (Ieda *et al.*, 1997). Another way of research concerns the modelling of the dynamics of space charge and field in insulating materials. This activity has suffered up to now from the absence of measured physical parameters describing the transport such as mobility, density, concentration of charges, etc. Some of these parameters could be extracted from the range of experiments that are now possible with the PEA (LeRoy *et al.*, 2004). Finally, on-line monitoring of the space charge in components and systems of electrical networks can be envisaged as well as diagnostic and prognostic based on relevant space charge quantity.

The use of complementary techniques, as it becomes now possible by PEA and current measurements for materials under field, and as it can be envisaged using in-situ PEA, surface potential and current measurements in materials under irradiation, certainly dispels a number of incertitude pertaining to techniques taken individually and opens the way to a reliable understanding of the behavior of materials. It also lets us foresee a major output which is forecasting their long-term behavior with the support of numerical modeling tools fed by the relevant physical hypotheses and appropriate parameterization.

5. Conclusion

This introduction to the PEA method we feel has confirmed the following properties: 1) This method is simple in its use and does not require a highly sophisticated mathematical treatment; 2) It gives consistent results as shown by the tests carried out under irradiation in which a known quantity of charge is implanted at a predetermined depth; 3) It allows the study of dynamic phenomena; 4) Then it can be used to study objects in which the space charges are generated by complex and uncontrolled processes.

6. Bibliography

Ahmed N. H., Srinivas N. N., "Review of space charge measurements in dielectrics", *IEEE Trans. Diel. & Elec. Insul.*, Vol. 4, 1997, p. 644-56.

Alison J. M., "A high field pulsed electro-acoustic apparatus for space charge and external circuit current measurement within solid insulators", *Meas. Sci. Technol.*, Vol. 9, 1998, p. 1737-1750.

Alison J. M., "The pulsed electro-acoustic method for the measurement of the dynamic space charge profile within insulators", *Space charge in solid dielectrics*, J. C. Fothergill and L. A. Dissado, Eds. Leicester, *The dielectrics Society*, 1998, p. 93-121.

Blaise G., Sarjeant W. J., "Space charge in dielectrics, Energy storage and transfer dynamics from atomistic to macroscopic scale", *IEEE Trans. Diel. & Elec. Insul.,* Vol. 5, 1998, p. 779-808.

Bloss P., Schafer H., "Investigations of polarization profiles in multilayer systems by using the laser intensity modulation method", *Rev. Sci. Instrum.*, Vol. 65, 1994, p. 1541-50.

Bloss P., Steffen M., Schafer H., Yang G. M., Sessler G. M., "A comparison of space-charge distributions in electron-beam irradiated FEP obtained by using heat-wave and pressure-pulse techniques", *J. Phys. D: Appl. Phys.*, Vol. 30, 1997, p. 1668-75.

Coelho R., Aladenize B., *Les diélectriques - Propriétés diélectriques des matériaux isolants*, Hermès, 1993.

Densley J., Hampton R. N., Henriksen M., Das-Gupta D. K., Toureille A., Hegerberg R., Takada T., Alquie C., Holboell J. T., Le-Gressus C., Gubenald S., Damanne G., Tanaka T., Nagao M., "Space charge measurements techniques: a review," *Electra/CIGRE*, Vol. 187, 1999, p. 74-89.

De Reggi A. S., Aimé S., "Experimental methods for dielectric polarization measurements", *Presented at Interdisciplinary Conference on Dielectrics Short Course*, 1992.

Dissado L. A., Mazzanti G., Montanari G. C., "The role of trapped space charges in the electrical ageing of insulating materials", *IEEE Trans. Diel. & Elec. Insul*, Vol. 4, 1997, p. 496-506.

Estar, "Electron Stopping power And Range", *software*, available at: http://physics.nist.gov/PhysRefData/Star/Text/ESTAR-u.html

Fukuma M., Nagao M., Kosaki M., Kohno Y., "Measurements of conduction current and electric field distribution up to electrical breakdown in LDPE films", *Proc. Conference on Electrical Insulation and Dielectric Phenomena*, Austin, Texas, October 17-20, 1999, p. 114-117.

Fukuma M., Nagao M., Hozumi N., Kosaki M., Kohno Y., Fukunaga K., Maeno T., "Development of very short interval space charge measurement system on PEA method", *Proc. Conference on Electrical Insulation and Dielectric Phenomena*, Cancun, Mexico, Oct. 20-24, 2002, p. 550-553.

Fukuma M., Maeno T., Fukunaga K., "Cross-section space charge measurement system," *Presented at ICSD*, Toulouse (France), 2004.

Fukunaga K., Maeno T., Okamoto K., "Space charge behaviour in the insulation layer of a metal-base printed wiring board", *Proc. International Conference on Conduction and Breakdown in Solid Dielectrics*, Vasteras, Sweden, June 1998, p. 102-105.

Fukunaga K., "Industrial applications of space charge measurement in Japan", *IEEE Electrical Insulation Magazine*, Vol. 15, No. 5, Sept./Oct.1999, p. 6-18.

Griseri V., Fukunaga K., Maeno T., Laurent C., Levy L., Payan D., "The pulsed electro-acoustic technique applied to in-situ measurement of charge distribution in electron-irradiated polymers", *IEEE Trans. Diel. & Elec. Insul.*, Vol. 11, 2004, p. 891-8.

Hozumi N., Takada T., Suzuki H., Okamoto K., "Direct observation of time-dependent space charge profiles in XLPE cable under high electric fields", *IEEE Trans. Diel. Elec. Insul.*, Vol. 1, 1994, p. 1068-1076.

Hozumi N., Muramoto Y., Nagao M., "Estimation of carrier mobility using space charge measurement technique", *Proc. Conference on Electrical Insulation and Dielectric Phenomena*, Austin, Texas, USA, 1999, p. 350-3.

Ieda M., Suzuoki Y., "Space charge and solid insulating materials: in pursuit of space charge control by molecular design", *IEEE Electrical Insulation Magazine*, Vol. 13, 1997, p. 10-17.

Jeroense M., *Charges and discharges in HVDC cables*, Delft University Press, 1997.

Kressmann R., Sessler G. M., Gunther P., "Space-charge electrets", *IEEE Trans. Diel. & Elec. Insul*, Vol. 3, 1996, p. 607-23.

Lang S. B., Das-Gupta D. K., "Laser-intensity-modulation method: a technique for determination of spatial distributions of polarization and space charge in polymer electrets", *J. Appl. Phys.*, Vol. 59, 1986, p. 2151-60.

Laurent C., "Diélectriques solides et charge d'espace", *Techniques de l'Ingénieur*, 1999, Chap. D2-305.

Laurenceau P., Dreyfus G., Lewiner J., "New principle for the determination of potential distributions in dielectrics", *Physical-Review-Letters*, Vol. 38, 1977, p. 46-9.

Le Roy S., Segur P., Teyssedre G., Laurent C., "Description of charge transport in polyethylene using a fluid model with a constant mobility: model prediction", *J. Phys. D. Appl. Phys.*, Vol. 37, 2004, p. 298-305.

Levy L., "Material charging", *Space environment: Prevention of risks related to spacecraft charging*, CNES/ONERA, Ed. Toulouse, Cépaduès, 2002, p. 241-265.

Li Y., Takada T., "Progress in space charge measurement of solid insulating materials in japan", *IEEE Elec. Insul. Magazine*, Vol. 10 (5), 1994, p. 16-28.

Li Y., Aihara M., Murata K., Tanaka Y., Takada T., "Space charge measurement in thick dielectric materials by pulsed electroacoustic method", *Rev. Sci. Instrum.*, Vol. 66, 1995, p. 3909-16.

Maeno T., Kushibe H., Tanaka T., Cooke C. M., "Pulsed elector-acoustic method for the measurement of volume charges in e-beam irradiated PMMA", *Presented at CEIDP*, 1985.

Maeno T., Fukunaga K., "High-resolution PEA charge distribution measurement system", *IEEE Trans. Diel. Elec. Insul.*, Vol. 3, 1996, p. 754-758.

Maeno T., Futami T., Kushibe H., Takada T., Cooke C. M., "Measurement of spatial charge distribution in thick dielectrics using the pulsed electroacoustic method", *IEEE Trans. Diel. & Elec. Insul.*, Vol. 23, 1988, p. 433-39.

Maeno T., "Calibration of pulsed electroacoustic method for measuring space charge density", *T. IEE Japan*, Vol. 119-A, 1999, p. 1114-19.

Maeno T., "Three dimensional space charge measurement system", *IEEE Trans. Diel. Elec. Insul.*, Vol. 8, 2001, p. 845-848.

Maeno T., Fukunaga K., "Open-PEA system for space charge measurement in dileectrics under irradiation", *Proc. International Conference on Solid Dielectrics*, Toulouse (France), 2004, p. 944-7.

Maeno T., "Portable space charge measurement system using the pulsed electroacoustic method", *IEEE Trans. Dielec. Elec. Insul.*, Vol. 10, No. 2, 2004, p. 331-336.

Miyake H., Le Roy S., Tanaka Y., Takada T., Teyssedre G., Laurent C., "Simultaneous measurement of electroluminescence and space charge distribution in cross-linked polyethylene under DC field", *Proc. International Conference on Solid Dielectrics,* Toulouse (France), 2004, p. 186-90.

Mizutani T., " Space charge measurement techniques and space charge in polyethylene", *IEEE Trans. Diel. & Elec. Insul.*, Vol. 1, 1994, p. 923-33.

Montanari G. C., Ghinello I., "Space charge and electrical conduction-current measurements for the inference of electrical degradation threshold", *Vide Science, Techniques et Applications.*, Vol. 287, 1998, p. 302-11.

Morshuis P., Jeroense M., "Space charge measurements on impregnated paper: a review of the PEA method and a discussion of results", *IEEE Elec. Insul. Magazine*, Vol. 13, 1997, p. 26-35.

Nothinger P., Toureille A., Santana J., Martinotto L., Albertini M., "Study of space charge accumulation in polyolefins submitted to ac stress", *IEEE Trans. Diel. Elec. Insul.*, Vol. 8, 2001, p. 972-984.

Nothinger P., Agnel S., Toureille A., "Thermal step method for space charge measurements under applied dc field", *IEEE Trans. Diel. Elec. Insul.*, Vol. 8, 2001, p. 985-994.

Satoh Y., Tanaka Y., Takada T., "Improvement of piezoelectrically induced PWP method and its comparison with the PEA method", *Elec. Eng. in Japan*, Vol. 121, 1997, p. 1-7.

Sessler G. M., "LIPP investigation of piezoelectricity distributions in PVDF poled with various methods", *Ferroelectrics*, Vol. 76, 1987, p. 489-96.

Sessler G. M., Alquie C., Lewiner J., "Charge distribution in Teflon FEP (fluoroethylenepropylene) negatively corona-charged to high potentials", *J. Appl. Phys.*, Vol. 71, 1992, p. 2280-4.

Sessler G. M., "Electrets: recent developments", *J. of Electrostatics*, Vol. 51-52, 2001, p. 137-45.

Takada T., "Acoustic and optical methods for measuring electric charge distributions in dielectrics", *IEEE Trans. Diel. & Elec. Insul.*, Vol. 6, 1999, p. 519-547.

Tardieu G., Apport des mesures de luminescence à la compréhension du piégeage et du transport dans les isolants synthétiques, Thèse, Toulouse, Université Paul Sabatier, 2003, p. 151.

Toureille A., Reboul J. P., "The thermal-step-technique applied to the study of charge decay in polyethylene thermoelectrets", *Presented at 6th International Symposium on Electrets ISE 6 Proceedings*, New York (USA), 1988.